REGULAR ARTICLE

Crystal Silicon Photoconductivity with Amorphous Inclusions

Oksana Babychenko[1],* ✉ iD, Olha Sushko[2], Serhii Babychenko[1],
Volodymyr Logunov[1], Hennadii Bendeberya[1]

[1] *Kharkiv National University of Radio Electronic, Microelectronics, Electronic Devices and Appliences Department, Kharkiv, Ukraine*
[2] *Kharkiv National University of Radio Electronic, Biomedical Engineering Department, Kharkiv, Ukraine*

The results of the numerical-analytical modeling of the photoconductivity of crystalline silicon with the inclusion of amorphous silicon are presented. These ones can be used in studying the principles of a new class of photovoltaic converters based on modified semiconductor materials. The initial data for such a model should be experimentally obtained layer parameters. During the calculations, it was assumed that the change in photoconductivity is caused by a change in the degree of disorder of amorphous inclusions. It was assumed that the semiconductor structure is dominated by cylindrical inclusions and the degree of sample disorder γ varies in the range from 0.040 to 0.065. That is, approximately 5 % of amorphous inclusions in the volume of the crystalline structure. The paper presents the results of calculations of changes in photoconductivity depending on the degree of disorder of the semiconductor structure. The results are in good agreement with obtained experimental data on amorphous-crystalline structures formed as a result of irradiation by γ-quanta. The photoconductivity of semiconductor samples irradiated with gamma rays was studied by microwave photomodulation methods using a resonator measuring transducer.

Keywords: Photoconductivity, Amorphous silicon, Disorder, Solar cell, Microwave cavity.

1. INTRODUCTION

A number of conditions are necessary for the effective operation of the solar cell (SC):

– the optical absorption coefficient of the active semiconductor layers should be sufficiently large to ensure that a significant part of the solar energy is absorbed within the thickness of the layers;

– electrons and holes generated in the illumination should be effectively assembled on contact electrodes;

– SC should have a significant energy barrier height;

– the full resistance, connected in series with the active element, must be small to reduce power losses [1-2].

The need to fulfill these requirements resulted in the use of a wide range of materials, technological and design solutions. Heterocompositions with thin and ultra-thin structures can be considered as a new class of semiconductor materials, the fundamental properties of which are determined by the type of structures, their thickness and the nature of the distribution of alloying impurities [3]. The structures formed on their basis will give an opportunity to control the charge carriers in the volume of the semiconductor.

In alloyed (*c-Si*)-semiconductor with a two-dimensional heterostructure the motion of nonequilibrium charge carriers is limited, they can move freely only along the plane of the layer. In the limiting case quantum well are formed at compatibility of two-dimensional heterostructures with a wavelength de Broglie charge carriers. One-dimensional heterostructures form quantum strands, in which charge carriers move only along them.

The combination of fundamental properties of direct zone (*a-Si*) and indirect zone (*c-Si*) structures in the single (*c-Si*)-matrix is the main difference from the existing devices developed on (*c-Si*) or (*a-Si*)-materials. In the structure (*c-Si*) charge carriers have high mobility ($\mu_n \sim 1500$, $\mu_p \sim 500$) cm²/V·s, but a low (except for the short-wave region of the solar spectrum) absorption coefficient of light. This cause makes use of large thicknesses of SC (≥ 100 μm).

In structure (*a-Si*), charge carriers have low drift mobility ($\mu_n \sim 10^{-1}$, $\mu_p \sim 10^{-3}$) cm²/V·s, but a significant absorption coefficient of light radiation, as well as a high concentration of recombination centers. These factors determine low efficiency of (*a-Si*)-SC.

2. RESULTS AND DISCUSSION

The main purpose of the work is comparing the theoretical calculated photoconductivity of an amorphous-crystalline silicon structure with experimental results obtained in the study of radiation defects accumulation in the volume of monocrystalline silicon with its irradiation with γ-quanta of braking radiation [4]. Microphotographs of the sample surface before and after irradiation with fragments of uranium fission and chemical etching are presented on (Fig. 1 a, b). On the surface of

---

* Correspondence e-mail: oksana.babychenko@nure.ua

the silicon plate there are undeveloped pores (craters) with a small number of pores going deep into the silicon wafer.

Figure 2a shows the structure of the cross section of the fragment of the silicon wafer after mechanical polishing, irradiation was carried out from the upper surface of the sample. A microstructure of silicon subjected to chemical etching is presented on Fig. 2b. The so-called etched pits formed on the cross-section of silicon samples, connected with the decay of violations of the crystalline structure, which are on the surface of monocrystalline silicon (dislocation outputs, inclusions of impurities, etc.). The place adjacent to the surface, which was irradiated by fragments of uranium, has a substantially higher density and the size of the etched pits. The thickness of this layer is from 5 to 30 microns.
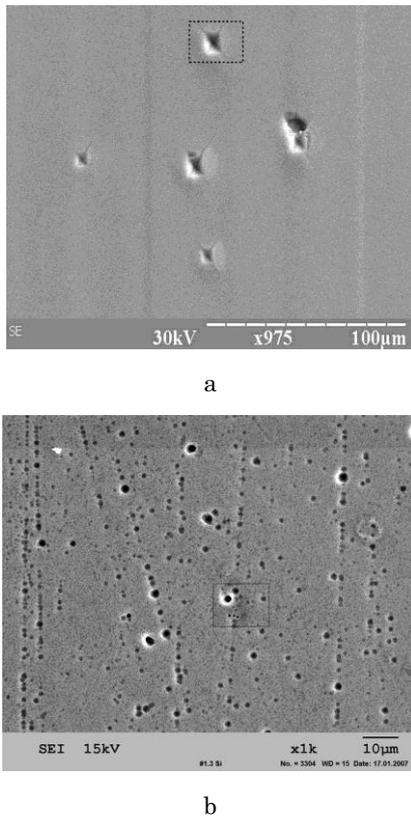

a

b

Fig. 1 – Microphotographs of the samples' surface before irradiation (a) after irradiation with fragments of uranium nuclei and etching (b)
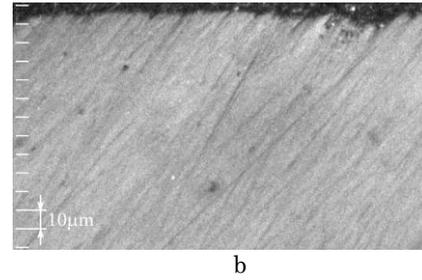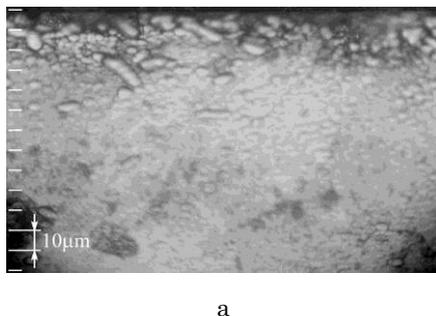

a

b

Fig. 2 – Microphotographs of the cross section of the sample after irradiation with uranium fragments

According to the results of the X-ray diffraction analysis, in the samples of monocrystalline silicon, the presence of some amount of amorphous phase formed as a result of their irradiation by fragments of the distribution of ^{238}U nuclei was established [4, 5].

Photoconductivity and lifetime of samples irradiated by gamma-quanta were investigated by microwave photo-modulation methods, which have the following advantages [6-7]:

– the operation without mechanical contact with the object of research;

– sensors' materials do not interact with the sample, which are in direct contact with its surface.;

– the lack of strict requirements for the geometry of the test material;

– the frequency of the resonator sensor depends only on the geometric dimensions of the last one;

– the microwave sensors are resistant to the environmental actions;

– the microwave electromagnetic waves do not destroy the test material;

– the microwave sensors are sensitive to changes in all characteristics of the test material.

A microwave cavity measuring transducer, which is a cylindrical cavity with H_{012} oscillation type, was used for the samples investigation.

The test sample, as schematically shown on Figure 3, is placed inside this cavity which is consisting of two coaxial parts perpendicular to its axis, completely covering the cross section of the cavity. The use of two pistons allows changing the location of the sample in the field of the measuring transducer in order to find the optimal level of its activation and obtain the maximum signal of photoconductivity at the output of the cavity.
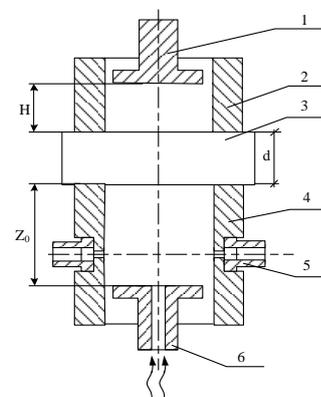

Fig. 3 – Measuring transducer's design. 1, 6 – adjustment pistons; 2, 4 – parts of cavity; 3 – sample; 5 – supply waveguides

Figure 4 shows the functional diagram of a microwave device for the investigation of photovoltaic properties of samples.

Figure 5 shows the measuring results of the photoconduction of Si sample after radiation processing and annealing for different radiation wavelengths (curve 1 – $\lambda = 0.57$ μm, curve 2 – $\lambda = 1$ μm).
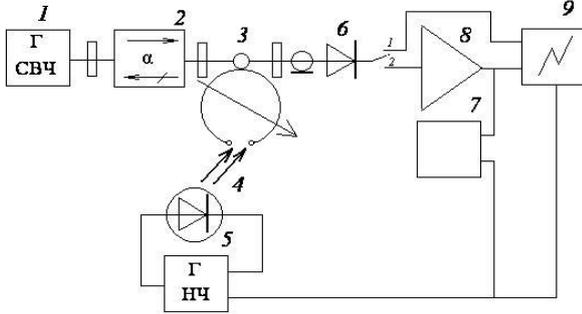

Fig. 4 – Functional diagram of the device for measuring the lifetime of charge carriers: 1 microwave generator, 2 – ferrite valve, 3 – microwave resonator, 4 – LED, 5 – special waveform generator, 6 – microwave diode, 7 – synchronous detector, 8 – selective amplifier, 9 – oscilloscope

The change in photoconductivity as a result of the annealing of the sample is due to a change in the structure of defects formed as a result of radiation processing of the sample and the restoration of torn bonds in the structure of amorphous inclusions.
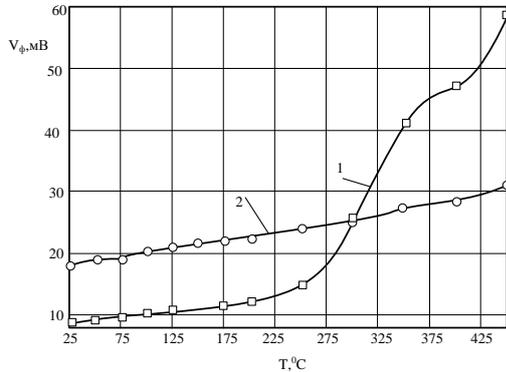

Fig. 5 – The dependence of *c-Si* sample photoconductivity after radiation processing on annealing temperature

Normalization of functional dependence on the magnitude of photoconductivity of the *c-Si* sample before its radiation processing is performed to determine the contribution to the photoconductivity of the structure of amorphous inclusions.

The value of the photoconductivity of the sample before the radiation processing is given in Table 1.

Table 1 – Photoconductivity of the sample before radiation processing

Side 1		Side 2	
V_0, mV ($\lambda = 1$ μm)	10.5	V_0, mV ($\lambda = 1$ μm)	1.93
V_0, mV ($\lambda = 0.57$ μm)	20.43	V_0, mV ($\lambda = 0.57$ μm)	3.05

Figure 6 shows the dependence of normalized photoconductivity for various wavelengths of radiation (1 – $\lambda = 1$ μm, b – $\lambda = 0.57$ μm).

The photoconductivity dependences are constructed for the theoretical description. The value of the photoconductivity appertained to the unit surface of the plate in the thickness d is equal

$$\sigma_{ph} = e \cdot \mu_n \cdot \Delta N, \qquad (1)$$
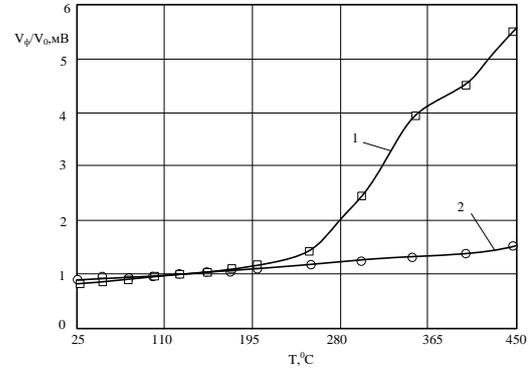
where

Fig. 6 – Dependencies of the normalized photoconductivity of the c-Si sample after radiation treatment depending on the annealing temperature

$$\Delta N = \frac{G \cdot \tau}{\alpha} \cdot \frac{1 - \exp(-\alpha d)}{1 + \frac{G \cdot \tau}{L} \cdot cth\left(\frac{d}{2 \cdot L}\right)} \times$$

$$\times \left[1 + \frac{G \cdot L}{D} \cdot \frac{\left[cth\left(\frac{d}{2 \cdot L}\right) - \alpha \cdot L \cdot cth\left(\frac{\alpha \cdot d}{2}\right) \right]}{1 - \alpha^2 \cdot L^2} \right].$$

The absorption coefficient α of three-phase system is a superposition of absorption coefficients of amorphous α_a, boundary α_{gb} and crystalline α_c phases and determined by the formula:

$$\alpha = X_g \cdot \alpha_c + X_{gb} \cdot \alpha_{gb} + (1 - X_c) \cdot \alpha_a. \qquad (2)$$

In the formula (2) X_g and X_{gb} are the particles of the crystalline phase and area of the partition boundary respectively. The absorption coefficient of boundary region α_{gb} is much more than α_a and α_c and increases with decreasing hydrogen concentration at the boundary. Since the size of the boundary is related to the concentration of hydrogen, then α_{gb} coefficient increases with the increase in the width of the boundary of the section. Consequently, the overall absorption coefficient of the structure increases. Under certain conditions hydrogen concentration decreases practically to zero, and the absorption coefficient of the boundary region reaches saturation. Since X_{gb} decreases, α absorption coefficient also decreases. With very large dimensions of the crystalline part of the structure, it approaches the absorption coefficient c-Si [8].

The absorption coefficient λ can be determined from the formula

$$\lambda(h\nu) = \frac{2 \cdot \pi \cdot h}{c} \cdot \left(\frac{q}{m}\right)^2 \times$$

$$\times \frac{1}{h\nu} \int N(E)f(E) \cdot N(E + h\nu)(1 - f(E_{h\nu}))P(E, E + h\nu)dE \qquad (3)$$

where hv is photon energy; z is refractive index; $N(E)$ is density of states; $f(E)$ is Fermi-Dirac distribution function; $P(E, E + hv)$ is matrix element of the optical transition. Thus, the contribution of states with E and $E + hv$ energies to the absorption coefficient is determined by the concentrations of filled output states with energy $E - N(E)f(E)$, empty final states with energy $E + hv - N(E + hv)(1 - f(E_{hv}))$ and the value of the matrix element of the transition from the initial to the final state $P(E, E + hv)$.

It is generally known that the state distribution reveals a quadratic dependence in the region of conduction (valence) and exponential dependence in the "tail" region but precise shape of the "tail" previously caused significant contradictions. It is also known that the transition of the function of the density of states between the zone and the region of the "tail" is smooth. The zones of the formation of "tails" are characterized by the width of the "tails" of the conduction band γ_c and the tails width of the valence band γ_v. These parameters of the tail width are a measure of disordered amorphous silicon. When allocating separate sections of the distribution of electronic states of "tails" and the stretching of all band states, one can assume that levels with energies

$$E_c + \frac{\gamma_c}{2} \text{ and } E_v - \frac{\gamma_v}{2}$$

represent the threshold of mobility of the conduction band and the valence band, respectively. Thus, the functions of the density of states for the conduction band and valence band have the form [9, 10]:

$$N_c(E) = \frac{\sqrt{2} \cdot m_c^{*3/2}}{\pi^2 \cdot \hbar^3} \begin{cases} \sqrt{E - E_c}, E \geq E_c + \frac{\gamma_c}{2} \\ \sqrt{\frac{\gamma_c}{2}} \cdot \exp\left(-\frac{1}{2}\right) \cdot \exp\left(\frac{E - E_c}{\gamma_c}\right), E < E_c + \frac{\gamma_c}{2}, \end{cases} \quad (4)$$

$$N_v(E) = \frac{\sqrt{2} \cdot m_v^{*3/2}}{\pi^2 \cdot \hbar^3} \begin{cases} \sqrt{\frac{\gamma_v}{2}} \cdot \exp\left(-\frac{1}{2}\right) \cdot \exp\left(\frac{E_v - E}{\gamma_v}\right), E \geq V_v - \frac{\gamma_v}{2} \\ \sqrt{E_v - E}, E < E_v - \frac{\gamma_v}{2}, \end{cases} \quad (5)$$

Where m_c^*, m_v^* is the effective mass of the electron in the conduction band and the effective mass of the hole in the valence band, respectively; E_c is energy of the bottom of the disordered conduction band; E_v is ceil of the disordered valence band. Results of calculations of the sensitivity of the functions of the states density of the conduction band and the valence band to the changes in γ_c and γ_v are presented on Fig. 7. The distribution of electronic states of "tails" appears below the mobility threshold for given values of γ_c. The total number of selected electron states of "tails" increases with increasing γ_v and the distribution of "tails" extends over a considerable distance in band gap. Similar results are observed for the function of the density of states of the valence band.

To determine the absorption coefficient it is assumed:

– the independence of the matrix element on energy, that is, its value is the same for all possible transitions in all of the considered spectral range;

– the refractive index does not depend on the photon energy;

– $f(E) = 1$ and $f(E + hv) = 0,$ that is, all the output states are filled with electrons and all final states are empty.

The results of calculating the spectral dependence of the absorption coefficient for different degrees of *a:Si: H* structure disordering and the value of the Taus width of the band gap 1.85 eV are given on Fig. 8. According to the dependency analysis, the degree of disordering affects significantly to the absorption coefficient of *a:*Si:H structure.
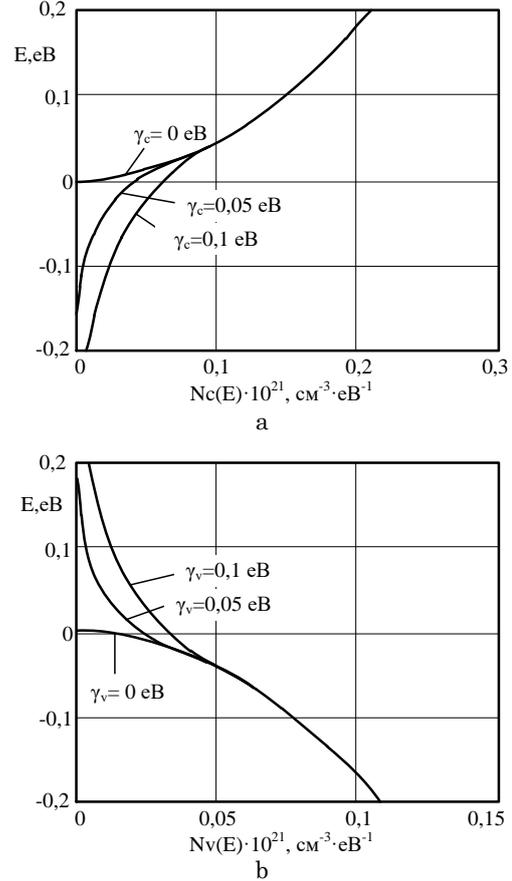

Fig. 7 – The dependence of the density of states for: a) the conduction band, b) the valence band
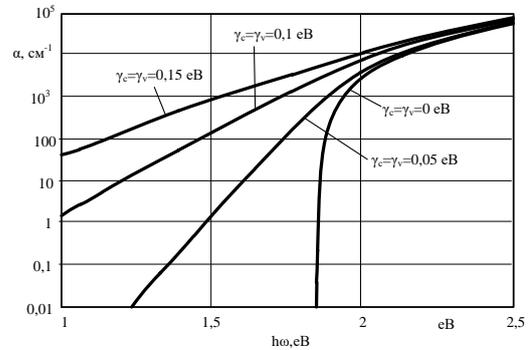

Fig. 8 – Spectral dependence of the absorption coefficient for the case at $\gamma_c = \gamma_v$ and $E_{g0} = 1.85$ eV
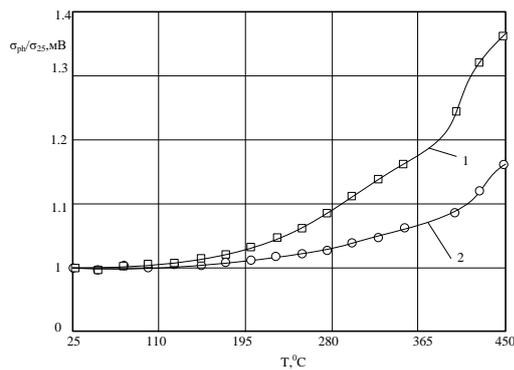
Fig. 9 – Results of the calculation of the relative change in photoconductivity

It is determined that the degree of disordering of the sample γ varies in the range from 0.04 to 0.065 [11] assuming that the structure is dominated by cylindrical inclusions. That is, about 5 % of amorphous inclusions are in the volume of crystalline structure.

The results of calculations according to the change in photoconductivity are shown on Figure 9. In calculations, it was assumed that the change in photoconductivity is due to a change in the degree of disordering of amorphous inclusions.

3. CONCLUSIONS

The obtained numerical-analytic results coincide with experimentally obtained results by the character of the curves change.

This indicates about the possibility of its application for optimization of structures and models of photo-transducers based on alloys of disordered and crystal-line silicon. Output data for this model should be exper-imentally obtained layers parameters. In addition, the model should allow solving the inverse problems for the purpose of extraction of the electrophysical parameters of the elements of the structure of the phototransducer from its experimental characteristics.

REFERENCES

1. A.R. Jha, *Solar Cell Technology and Applications* (Taylor and Francis Group: 2010).
2. A.B. Galat, *Telecommunications and Radio Engineering* **74** No 13, 1215 (2015).
3. O.A. Sushko, M.M. Rozhitskii, *J. Nano- Electron. Phys.* **6** No 1, 01009 (2014).
4. A.N. Dovbnya, V.P. Yefimov, G.D. Pugachev, V.S. Dyomin, N.A. Dovbnya, J.E. Gordienko, B.G. Borodin, S.V. Babychenko, T.A. Semenets, *Probl. At. Sci. Technol. Series: Nuclear Physics Investigations*. **3** No 47, 179 (2006).
5. A.N. Dovbnya, V.P. Yefimov, H.D. Pugachev, V.S. Dyomin, N.A. Dovbnya, J.E. Gordienko, B.H. Borodin, S.V. Babychenko, T.A. Semenets, *Novi Tekhnolohiyi* No 1-2 (7–8) (2005) [In Ukrainian].
6. A. Bilotserkivska, I. Bondarenko, A. Gritsunov, O. Babychenko, L. Sviderska, A. Vasianovych, *Proc. 2022 IEEE 2nd Ukrainian Microwave Week (UkrMW-2022)* (Ukraine, Kharkiv: 2022).
7. I.N. Bondarenko, I.Yu. Bliznyuk, E.A. Gorbenko, *Tele-communications and Radio Engineering* **78** No 5, 385 (2019).
8. F. Diehl, M. Scheib, B. Schroder, H. Oechsner, *J. Non-Cryst. Solids* **227-230**, 973 (1998).
9. O.Y. Babychenko, A.G. Pashchenko, *J. Nano- Electron. Phys.* **9** No 5, 05044 (2017).
10. O.Yu. Sologub, *23rd International Crimean Conference Microwave and Telecommunication Technology (CriMiCo-2013)*, art. no.6653046, (Sevastopol: Veber: 2013).
11. A.G. Pashchenko, O.Yu. Sologub, *Telecommunications and Radio Engineering* **73** No 5, 447 (2014).

Фотопровідність кристалічного кремнію з аморфними включеннями

Оксана Бабиченко[1], Ольга Сушко[2], Сергій Бабиченко[1], Володимир Логунов[1], Геннадій Бендеберя[1]

[1] *Харківський національний університет радіоелектроніки, кафедра мікроелектроніки, електронних при-ладів та пристроїв, Харків, Україна*
[2] *Харківський національний університет радіоелектроніки, кафедра біомедичної інженерії, Харків, Україна*

Представлені результати чисельно-аналітичного моделювання фотопровідності кристалічного кремнію з включеннями аморфного кремнію, які можуть бути використані при вивченні принципів роботи нового класу фотоелектричних перетворювачів на основі модифікованих напівпровідникових матеріалів. Вихідними даними для такої моделі мають бути експериментально отримані параметри шарів. При розрахунках припускалось, що зміна фотопровідності обумовлена зміною ступеня розупо-рядкованості аморфних включень. Було зроблене припущення, що в напівпровідниковій структурі домінують циліндричні включення та ступінь розупорядкованості зразка γ змінюється в діапазоні від 0.040 до 0.065. Тобто в об'ємі кристалічної структури приблизно 5 % аморфних включень. У роботі наведені результати розрахунків зміни фотопровідності в залежності від ступеню розупорядковано-сті напівпровідникової структури. Результати співпадають з раніше отриманими експериментальни-ми даними на аморфно-кристалічних структурах, утворених в результаті опромінення γ-квантами. Фотопровідність напівпровідникових зразків опромінених гамма-квантами досліджувалися НВЧ фо-томодуляційними методами за допомогою резонаторного вимірювального перетворювача.

Ключові слова: Фотопровідність, Аморфний кремній, Розупорядкованість, Сонячний елемент, НВЧ резонатор.